

Constraints of Perception and Cognition in Relativistic Physics

Manoj Thulasidas

*Neural Signal Processing Lab, Institute for Infocomm Research,
National University of Singapore, 21 Heng Mui Keng Terrace, Singapore 119613.**

(Dated: November 20, 2018)

Cognitive neuroscience treats reality as our brain's representation of our sensory inputs. In this view, our perceptual reality is only a distant and convenient mapping of the physical processes causing the sensory inputs. Sound is a mapping of auditory inputs, and space is a representation of visual inputs. Any limitation in the chain of sensing has a specific manifestation on the cognitive representation that is our perceived reality. One physical limitation of our visual sensing is the finite speed of light. The manifestation of this limitation is the reason why the speed of light appears at the basic structure of our space-time. Physics, however, treats the perceptual reality of space and time (our brain's representation) as a faithful image of the physical reality (the objects and phenomena causing the sensory inputs). This faith in our cognitive map or perceived reality results in attributing the manifestations of the limitations of our perception to the true nature of space and time. In this article, we look at the consequences of the limited speed of our perception, namely the speed of light, and show that they are remarkably similar to the coordinate transformation in the special theory of relativity. Further illustrating the validity of looking at the visual reality as our brain's representation limited by the speed of light, we show that we can unify and explain a wide array of seemingly unrelated astrophysical and cosmological phenomena using this framework. Understanding the constraints on our space and time due to the limitations in perception and cognitive representation opens the possibility of understanding astrophysics and cosmology from a whole new viewpoint.

PACS numbers: 95.30.-k, 98.80.Jk, 98.62.Nx, 98.70.Rz, 98.70 Vc

Keywords: cognitive neuroscience; reality; special relativity; light travel time effect; gamma rays bursts; cosmic microwave background radiation.

I. INTRODUCTION

Our reality is a mental picture that our brain creates, starting from our sensory inputs [1]. Although this cognitive map is often mistaken to be a faithful image of the physical causes behind the sensing process, the causes themselves are very different from the perceptual experience of sensing. The difference between the cognitive representation and their physical causes is not immediately obvious when we consider our primary and most powerful sense of sight. But, we can appreciate the difference by looking at our less powerful olfactory and auditory senses. Odors, which may appear to be a property of the air we breathe, are in fact our brain's representation of the chemical signatures that our nose senses. Similarly, sound is not an intrinsic property of a vibrating body, but our brain's mechanism to represent the pressure waves in the air. Table I shows the chain from the physical cause of the sensory input to the final reality as the brain creates it. Although the physical causes can be identified for olfactory and auditory chains, they are not easily discerned for visual process. Since sight is the most powerful sense we possess, we are obliged to accept our brain's representation of visual inputs as the fundamental reality.

A good indication of the tight integration between the

Sense modality	Physical cause	Sensing signal	Brain's representation
Olfactory	Chemicals	Chemical concentrations	Smells
Auditory	Vibrating objects	Air pressure waves	Sounds
Visual	Unknown	Light	Space, time reality

TABLE I: Brain's representation of different sensory inputs. Odors are a representation of chemical compositions and concentration our nose senses. Sounds are a mapping of the air pressure waves produced by a vibrating object. In sight, we do not know the physical reality, our representation is space, and possibly time.

physiology of perception and its representation in the brain was proven recently [2] in a clever experiment using the tactile funneling illusion. This illusion results in a single tactile sensation at the focal point at the center of a stimulus pattern even though no stimulation is applied at that site. In the experiment, the brain activation region corresponded to the focal point where the sensation was perceived rather than the points where the stimuli were applied, proving that brain registered perceptions, not the physical causes of the perceived reality. In other words, for the brain, there is no difference between applying the pattern of the stimuli and applying just one stimulus at the center of the pattern. Brain maps the sensory inputs to regions that correspond to

*Electronic address: manoj@i2r.a-star.edu.sg

their perception, rather than the regions that physiologically correspond to the sensory stimuli.

The neurological localization of different aspects of reality has been established by lesion studies in neuroscience. The perception of motion (and the consequent basis of our sense of time), for instance, is so localized that a tiny lesion can erase it completely. Cases of patients with such specific loss of a part of reality [1] illustrate the fact that our experience of reality, every aspect of it, is indeed a creation of the brain. Space and time are aspects of the cognitive representation in our brain.

Space is a perceptual experience much like sound. Comparisons between the auditory and visual modes of sensing can be useful in understanding the limitations of their representations in the brain. One limitation is the input ranges of the sensory organs. Ears are sensitive in the frequency range 20Hz–20kHz, and eyes are limited to the visible spectrum. Another limitation, which may exist in specific individuals, is an inadequate representation of the inputs. Such a limitation can lead to tone-deafness and color-blindness, for instance. The speed of the sense modality also introduces an effect, such as the time lag between seeing an event and hearing the corresponding sound. For visual perception, the consequence of the finite speed of light is called the light travel time effect, which offers a convincing explanation to the observed superluminal motion in certain celestial objects [3, 4]. When an object approaches the observer at a shallow angle, the transverse speed may appear superluminal.

However, other consequences of the light travel time (LTT) effect are very similar to the coordinate transformation of the special theory of relativity (SR). These consequences include an apparent contraction of a receding object along its direction of motion and a time dilation effect. Furthermore, a receding object can never *appear* to be going faster than the speed of light, even if its real speed is superluminal. While SR does not explicitly forbid it, superluminality is understood to lead to time travel and the consequent violations of causality. An *apparent* violation of causality is one of the consequences of LTT, when the superluminal object is approaching the observer. All these effects due to LTT are remarkably similar to SR. However, LTT effects are currently assumed to apply on a space-time that obeys SR. It may be that there is a deeper structure to the space-time, of which SR is only our perception, filtered through LTT effect. By treating LTT effects as an optical illusion to be applied on an SR-like space-time, we may be double counting them.

Once we accept the neuroscience view of reality as a representation of our sensory inputs, we can understand why the speed of light figures so prominently in our physical theories. The theories of physics are a description of reality. Reality is created out of the readings from our senses, especially our eyes. They work at the speed of light. Thus the sanctity accorded to the speed of light is a feature only of *our* reality, not the absolute, ultimate reality which our senses are striving to perceive. When it

comes to physics that describes phenomena well beyond our sensory ranges, we really have to take into account the role that our perception and cognition play in seeing them. The universe as we see it is only a cognitive model created out of the photons falling on our retina or on the photo-sensors of the Hubble telescope. Because of the finite speed of the information carrier (namely photons), our perception is distorted in such a way as to give us the impression that space and time obey special relativity. They do, but space and time are not the absolute reality. “Space and time are modes by which we think and not conditions in which we live,” as Einstein himself put it.

Treating our perceived reality as our brain’s representation of our visual inputs (filtered through the light travel time effect), we will see that all the strange effects of the coordinate transformation in special relativity can be understood as the manifestations of the finite speed of our senses in our space and time. Furthermore, this line of thinking leads to natural explanations for two classes of astrophysical phenomena:

Gamma Ray Bursts currently believed to emanate from cataclysmic stellar collapses, and

Radio Sources considered manifestations of space-time singularities or neutron stars.

Beyond unifying these apparently distinct astrophysical phenomena, the cognitive limitations to reality can provide qualitative explanations for such cosmological features as the apparent expansion of the universe and the Cosmic Microwave Background Radiation (CMBR). Both these phenomena can be understood as related to our perception of superluminal objects. It is the unification of these seemingly distinct phenomena at vastly different length and time scales, along with its conceptual simplicity, that we hold as the indicators of validity of this framework.

II. SIMILARITIES BETWEEN LTT EFFECTS AND SR

The coordinate transformation derived in the original paper [5] is, in part, a manifestation of light travel time (LTT) effects. This is most obvious in the first thought experiment, where observers moving with a rod find their clocks not synchronized due to the difference in light travel times along the length of the rod. In this section, we will consider space and time as a part of the cognitive model created by the brain, and illustrate that special relativity applies to the cognitive model. The absolute reality (of which the SR-like space-time is our perception) does not have to obey the restrictions of SR. In particular, objects are not restricted to subluminal speeds, but they may appear to us as though they are restricted to subluminal speeds in our perception of space and time. If we disentangle LTT effects from the rest of

SR, we can understand a wide array of phenomena, as we shall see in this article. Although not attempted in this paper, the primary motivation for SR, namely the covariance of Maxwell's equations, may be accomplished even without attributing LTT effects to the properties of space and time.

A feature of SR is that it seeks a linear coordinate transformation between coordinate systems in motion with respect to each other. We can trace the origin of linearity to a hidden assumption on the nature of space and time built into SR, as stated by Einstein [5]: "In the first place it is clear that the equations must be linear on account of the properties of homogeneity which we attribute to space and time." Because of this assumption of linearity, the original derivation of the transformation equations ignores the asymmetry between approaching and receding objects. Both approaching and receding objects can be described by two coordinate systems that are always receding from each other. For instance, if a system K is moving with respect to another system k along the positive X axis of k , then an object at rest in K at a positive x is receding while another object at a negative x is approaching an observer at the origin of k . Unlike SR, considerations based on LTT effects result in intrinsically different set of transformation laws for objects approaching an observer and those receding from him. More generally, the transformation depends on the angle between the velocity of the object and the observer's line of sight. Since the transformation equations based on LTT effects treat approaching and receding objects asymmetrically, they provide a natural solution to the twin paradox, for instance.

A. Perception of Speed

We first look at how the perception of motion is modulated by the light travel time (LTT) effects. As remarked earlier, the transformation equations of SR treat only objects receding from the observer. For this reason, we first consider a receding object, flying away from the observer at a speed $\beta = v/c$, where c is the speed of light. The apparent speed β_o of the object depends on the real speed β (as shown in Appendix A 1):

$$\beta_o = \frac{\beta}{1 + \beta}$$

$$\lim_{\beta \rightarrow \infty} \beta_o = 1$$

Thus, due to LTT effects, an infinite real velocity gets mapped to an apparent velocity $\beta_o = 1$. In other words, no object can appear to travel faster than the speed of light, entirely consistent with SR.

Physically, this apparent speed limit amounts to a mapping of c to ∞ , which is most obvious in its consequences. For instance, it takes an infinite amount of energy to accelerate an object to an apparent speed $\beta_o = 1$, because, in reality, we are accelerating it to an

infinite speed. This infinite energy requirement can also be viewed as the relativistic mass changing with speed, reaching ∞ at $\beta_o = 1$. Einstein explained this mapping as: "For velocities greater than that of light our deliberations become meaningless; we shall, however, find in what follows, that the velocity of light in our theory plays the part, physically, of an infinitely great velocity." Thus, for objects receding from the observer, the effects of LTT are almost identical to the consequences of SR, in terms of the perception of speed.

B. Time Dilation

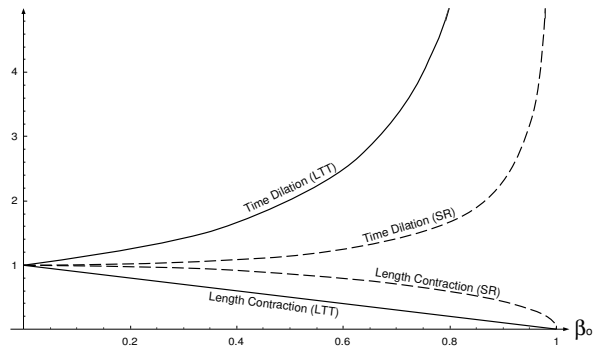


FIG. 1: Comparison between light travel time (LTT) effects and the predictions of the special theory of relativity (SR). The X-axis is the apparent speed and the Y-axis shows the relative time dilation or length contraction.

LTT effects influence the way time at the moving object is perceived. Imagine an object receding from the observer at a constant rate. As it moves away, the successive photons emitted by the object take longer and longer to reach the observer, because they are emitted at farther and farther away. This travel time delay gives the observer the illusion that time is flowing slower for the moving object. It can be easily shown (see Appendix A 2) that the time interval observed Δt_o is related to the real time interval Δt as:

$$\frac{\Delta t_o}{\Delta t} = \frac{1}{1 - \beta_o}$$

for an object receding from the observer ($\theta = \pi$). This observed time dilation is plotted in figure 1, where it is compared to the time dilation predicted in SR. Note that the time dilation due to LTT is stronger than the one predicted in SR. However, the variation is similar, with both time dilations tending to ∞ as the observed speed tends to c .

C. Length Contraction

The length of an object in motion also appears different due to LTT effects. It can be shown (see Appendix A 3)

that observed length d_o is related to the real length d as:

$$\frac{d_o}{d} = 1 - \beta_o$$

for an object receding from the observer with a speed of β_o . This equation also is plotted in figure 1. Note again that the LTT effects are stronger than the ones predicted in SR.

Figure 1 illustrates that both time dilation and Lorentz contraction can be thought of as LTT effects. While the actual magnitudes of LTT effects are larger than what SR predicts, their qualitative behavior as a function of speed is very similar. This similarity is not surprising because the coordinate transformation in SR is partly based on light travel time effects. If LTT effects are to be applied, as an optical illusion, on top of the consequences of SR as currently believed, then the total observed length contraction and time dilation will be significantly more than SR predictions.

D. Doppler Shift

The Doppler shift is one of the few dynamic properties of a celestial object that we can measure directly. The measured redshift is easily translated to a speed, yielding a view of an expanding universe. As shown in Appendix A 4, the redshift $1 + z$ depends on the real and apparent speeds as follows:

$$\begin{aligned} 1 + z &= \frac{1}{1 + \beta_o \cos \theta} \\ &= 1 - \beta \cos \theta \end{aligned}$$

where β is the real speed of the object, and β_o is its apparent speed. For a receding object ($\theta = \pi$) moving at subluminal speeds ($\beta < 1$), we can rewrite this equation as:

$$1 + z = \sqrt{\frac{1 + \beta}{1 - \beta_o}}$$

If we were to mistakenly assume that the speed we observe is the real speed, then this becomes the familiar relativistic Doppler shift formula:

$$1 + z = \sqrt{\frac{1 + \beta}{1 - \beta}}$$

While it is interesting that we get the relativistic Doppler shift formula, it should be noted that setting $\beta_o = \beta$ breaks down the derivation of these equations. However, this similarity in the forms of the final equations is indicative of the common basis in their origin.

III. LTT EFFECTS FOR APPROACHING OBJECTS

A. Asymmetric Effects

One important feature of LTT effects is that they are asymmetric in their dependence on speed; β and β_o appear in odd power, so that the equations are odd. More generally, there is a term involving the angle θ between the object's velocity and the observer's line of sight. In SR, on the other hand, β almost always appears as β^2 and the equations are even. SR treats the effect of motion as a linear coordinate transformation, ignoring the angle. Thus, in SR, the effect is the same whether the object is approaching or receding from the observer. As remarked before, this fundamental difference can be traced back to the assumed homogeneity of space and time in SR. The asymmetry in LTT effects, on the other hand, provides convincing explanations to certain paradoxes: the twin paradox, the observed superluminal motion, the causality violation due to superluminal motion etc. At the same time, the asymmetry makes it difficult to reconcile LTT effects and SR completely.

B. Time Contraction and Length Expansion

The asymmetric consequences of LTT effects include an apparent time contraction. When an object is approaching the observer, the time at the object seems to flow at an accelerated rate for the observer. This effect is easy to understand because, as the object is approaching the observer, the successive photons are emitted at shorter and shorter distances and they take less and less time to reach the observer, creating an illusion of an accelerated time flow, or time contraction.

By the same argument, the moving object appears elongated along the direction of motion as it is flying towards the observer. Appendices A 2 and A 3 show the mathematical details of how light travel time effects result in an apparent time contraction and length expansion. If Δt_o is the apparent time duration as felt by the observer and Δt is the real time, then:

$$\frac{\Delta t_o}{\Delta t} = \frac{1}{1 + \beta_o}$$

Similarly, an object of real length d appears to have an elongated length d_o as given by:

$$\frac{d_o}{d} = 1 + \beta_o$$

IV. EXPLANATIONS BASED ON LIGHT TRAVEL TIME EFFECT

A. Twin Paradox

The famous twin paradox in SR exploits the symmetry in its coordinate transformation. In this paradox, one twin goes away to a galaxy far away, accelerating to speeds close to c . The other one stays back on earth. When the traveling twin comes back (again accelerating to almost c on the way), he will be much younger than the twin that stays back, due to time dilation. But, in the traveling twin's frame of reference, it is the other twin (along with the earth) that is traveling at speeds close to c . Thus, time dilation should apply to the one that stays back. This paradox is resolved by arguing that the traveling twin feels the tremendous acceleration and deceleration, and his frame of reference is not an inertial frame.

In the LTT picture, the time dilation equation is asymmetric. Whatever time dilation one twin seems to feel on the way out is compensated by an exactly same amount of contraction on his way back. Thus, to each of the twins, the other twin seems to be enjoying the benefits of time dilation and aging slower. But, this time dilation happens only during the outward journey, when the twins are going away from each other. On his way back, the traveling twin will see the other twin aging much faster. At the same time, to the twin that stays back, the traveling twin will appear to be aging much faster. When they meet again, there will not be any age difference.

B. Superluminality and Causality

Although superluminality is generally believed to lead to time travel and the consequent causality violations, SR does not explicitly state this. As quoted earlier, Einstein merely remarked that “our deliberations become meaningless” at superluminal speeds. In any case, we saw that for a receding object, the apparent speed could never be superluminal. And SR considers only receding frames of reference. In our derivations of LTT effects on length contraction and time dilation, we did not impose the condition that $\beta < 1$.

Using our equation for time dilation, for an approaching object, $\theta = 0$.

$$\frac{\Delta t_o}{\Delta t} = 1 - \beta$$

Thus, if the object is flying to the observer, up to the speed of light ($0 < \beta < 1$), the time intervals appear shorter and shorter. When the speed of approach exceeds c , the *apparent* time flows backwards. This is because a photon emitted at a particular point along the trajectory reaches the observer *before* a photon emitted earlier and farther away. The order in which photons emitted by the object reach the observer is reversed. This reversal of

time flow will give rise to an apparent violation of causality. This violation of causality is only an LTT effect (akin to a video clip playing backwards), not a fundamental property of space and time as currently believed. Note, however, that astrophysical causality violations may not be obvious. For instance, imagine a cataclysmic explosion of a star and a subsequent fireball. This scenario played backwards would be a imploding fireball and an appearance of a star. We may think of it as the accretion of matter by an invisible massive object or the birth of a star, instead of an event showing causality violation.

C. Apparent Superluminal Motion

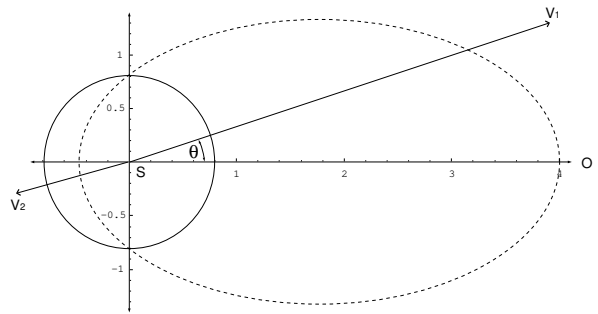


FIG. 2: Illustration of the traditional explanation for the apparent superluminal motion. An object expanding at a speed $\beta = 0.8$, starting from a single point S. The solid circle represents the boundary one second later. The observer is far away on the right hand side, O ($x \rightarrow \infty$). The dashed ellipse is the apparent boundary of the object, as seen by the observer.

We can measure the transverse velocity of a celestial object almost directly using angular measurements, which are translated to a speed using its known (or estimated) distance from us. In the past few decades, scientists have observed [3, 4] objects moving at apparent transverse velocities significantly higher than the speed of light. Some such superluminal objects were detected within our own galaxy [6, 7, 8, 9]. Rees [10] offered an explanation why such apparent superluminal motion is not in disagreement with SR based on LTT effects, even before the phenomenon was discovered.

The distortion in the perception of speed, when the object is approaching the observer, is used to explain the apparent superluminal motion. Figure 2 illustrates the explanation of apparent superluminal motion as described in the seminal paper by Rees [10]. In this figure, the object at S is expanding radially at a constant speed of $0.8c$, a highly relativistic speed. The part of the object expanding along the direction V_1 , close to the line of sight of the observer, will appear to be traveling much faster. This will result in an apparent transverse velocity that can be superluminal.

Imagine an object in motion at a speed β . To an observer, it appears to move with a speed of β_o . The ap-

parent speed β_o of the object depends on the real speed β and the angle between its direction of motion and the observer's line of sight, θ . As shown in Appendix A 1,

$$\beta_o = \frac{\beta}{1 - \beta \cos \theta} \quad (1)$$

Figure 2 is a representation of equation (1) as $\cos \theta$ is varied over its range. It is the locus of β_o for a constant $\beta = 0.8$, plotted against the angle θ . The apparent speed is in complete agreement with what was predicted in 1966 (Figure 1 in the original article, Rees [10]).

For a narrow range of θ , the transverse component of the apparent velocity ($\beta_o \sin \theta$) can appear superluminal. From equation (1), it is easy to find this range:

$$\frac{1 - \sqrt{2\beta^2 - 1}}{2\beta} < \cos \theta < \frac{1 + \sqrt{2\beta^2 - 1}}{2\beta} \quad (2)$$

Thus, for appropriate values of $\beta (> \frac{1}{\sqrt{2}})$ and θ (as given in equation (2)), the transverse velocity of an object can seem superluminal, even when the real speed is in conformity with the special theory of relativity.

While equations (1) and (2) explain the apparent transverse superluminal motion the difficulty arises in the recessional side. Along directions such as V_2 in figure 2, the apparent velocity is always smaller than the real velocity. It can be shown that the apparent velocity of the slower jet can never be more than the reciprocal of the faster jet, if the real speeds are to be subluminal. This calculation is shown in Appendix sec:jet. Thus, superluminality can never be observed in both the jets of a radio source, which indeed has not been reported so far. Near exact symmetry in extragalactic radio sources, including subluminal jets, is also qualitatively inconsistent with this explanation.

D. Symmetric Radio Sources

If we accept that special relativity applies to our cognitive map of reality or the perceived space and time, and that the absolute reality, of which space and time are our perception, is free of the constraints of SR, we can find elegant descriptions of symmetric radio sources and jets. Different classes of such objects associated with Active Galactic Nuclei (AGN) were found in the last fifty years. The radio galaxy Cygnus A [11], one of the brightest radio objects, is an example of such a radio source. Many of its features are common to most extragalactic radio sources: the symmetric double lobes, an indication of a core, an appearance of jets feeding the lobes and the hotspots. Owsianik and Conway [12] and Polatidis et al. [13] have reported more detailed kinematical features, such as the proper motion of the hotspots in the lobes. Here, we show that our perception of an object crossing our field of vision at a constant superluminal speed is remarkably similar to a pair of symmetric

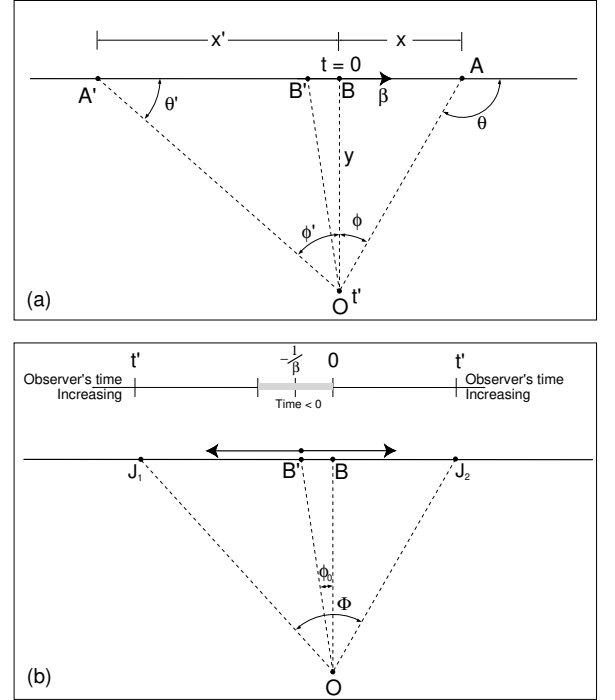


FIG. 3: The top panel (a) shows an object flying along $A-B-A$ at a constant superluminal speed. The observer is at O . The object crosses B (the point of closest approach to O) at time $t = 0$. The bottom panel (b) shows how the object is perceived by the observer at O . It first appears at B' , then splits into two. The two apparent objects seem to go away from each other (along J_1 and J_2) as shown.

hotspots departing from a fixed point with a decelerating rate of angular separation.

Consider an object moving at a superluminal speed as shown in figure 3(a). The point of closest approach is B . At that point, the object is at a distance of y from the observer at O . Since the speed is superluminal, the light emitted by the object at some point B' (before the point of closest approach B) reaches the observer *before* the light emitted at A . This reversal creates an illusion of the object moving in the direction from B' to A , while in reality it is moving in the opposite direction.

We use the variable t_o to denote the observer's time. Note that, by definition, the origin in the observer's time axis is set when the object appears at B . ϕ is the observed angle with respect to the point of closest approach B . ϕ is defined as $\theta - \pi/2$ where θ is the angle between the object's velocity and the observer's line of sight. ϕ is negative for negative time t .

As shown in Appendix A 5, a relation between t_o and ϕ can be readily derived.

$$t_o = y \left(\frac{\tan \phi}{\beta} + \frac{1}{\cos \phi} - 1 \right) \quad (3)$$

Here, we have chosen units such that $c = 1$, so that y

is also the time light takes to traverse BO . The origin of the observer's time is set when the observer sees the object at B . i.e., $t_o = 0$ when the light from the point of closest approach B reaches the observer.

The actual plot of ϕ as a function of the observer's time is given in figure 4 for different speeds β . Note that for subluminal speeds, there is only one angular position for any given t_o . For subluminal objects, the observed angular position changes almost linearly with the observed time, while for superluminal objects, the change is parabolic. The time axis scales with y .

Equation (3) can be approximated using a Taylor series expansion as:

$$t_o \approx y \left(\frac{\phi}{\beta} + \frac{\phi^2}{2} \right) \quad (4)$$

From the quadratic equation (4), one can easily see that the minimum value of t_o is $t_{o\min} = -y/2\beta^2$ and it occurs at $\phi_0 = -1/\beta$. Thus, to the observer, the object first appears (as though out of nowhere) at the position ϕ_0 at time $t_{o\min}$. Then it appears to stretch and split, rapidly at first, and slowing down later.

The angular separation between the objects flying away from each other is:

$$\Phi = \frac{2}{\beta} \sqrt{1 + \frac{2\beta^2}{y} t_o} = \frac{2}{\beta} (1 + \beta\phi)$$

And the rate at which the separation occurs is:

$$\frac{d\Phi}{dt_o} = \sqrt{\frac{2}{yt_{\text{age}}}} = \frac{2\beta}{y(1 + \beta\phi)}$$

where $t_{\text{age}} = t_o - t_{o\min}$, the apparent age of the symmetric object. (The mathematical details can be found in Appendix A 5.)

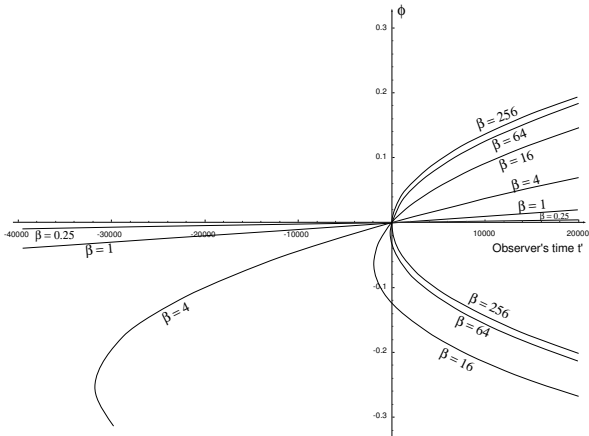


FIG. 4: The apparent angular positions of an object traveling at different speeds at a distance y of one million light years from us. The angular positions (ϕ in radians) are plotted against the observer's time t_o in years.

This discussion shows that a single object moving across our field of vision at superluminal speed creates an illusion of an object appearing at a certain point in time, stretching and splitting into two and then moving away from each other. This time evolution of the two objects is given in equation (3), and illustrated in the bottom panel of figure 3(b). Note that the apparent time t_o (as perceived by the observer) is reversed with respect to the real time t in the region A_- to B' . An event that happens near B' appears to happen before an event near A_- . Thus, the observer may see an apparent violation of causality, but it is just a part of the light travel time effect.

If there are multiple objects, moving as a group, at roughly constant superluminal speed along the same direction, they will appear as a series of objects materializing at the same angular position and moving away from each other sequentially, one after another. The apparent knot in one of the jets always has a corresponding knot in the other jet.

E. Redshifts of the Hotspots

In the previous section, we showed how a superluminal object appears as two objects receding from a core. Now we consider the time evolution of the redshift of the two apparent objects (or hotspots). Since the relativistic Doppler shift equation is not appropriate for our considerations, we need to work out the relationship between the redshift (z) and the speed (β) from first principles. This calculation is done in Appendix A 4:

$$\begin{aligned} 1 + z &= |1 - \beta \cos \theta| \\ &= |1 + \beta \sin \phi| \\ &= \left| 1 + \frac{\beta^2 t}{\sqrt{\beta^2 t^2 + y^2}} \right| \end{aligned} \quad (5)$$

We can explain the radio frequency spectra of the hotspots as extremely redshifted black body radiation, because β can be very large in our model of extragalactic radio sources. Note that the limiting value of $|1 + z|$ is roughly β , which gives an indication of the speeds required to push the black body radiation to RF spectra. Since the speeds (β) involved are typically very large, and we can approximate the redshift as:

$$1 + z \approx |\beta\phi| \approx \frac{|\beta\Phi|}{2}$$

Assuming the object to be a black body similar to the sun, we can predict the peak wavelength (defined as the wavelength at which the luminosity is a maximum) of the hotspots as:

$$\lambda_{\max} \approx (1 + z)480\text{nm} \approx \frac{|\beta\Phi|}{2}480\text{nm}$$

where Φ is the angular separation between the two hotspots.

This equation shows that the peak RF wavelength increases linearly with the angular separation. If multiple hotspots can be located in a twin jet system, their peak wavelengths will depend only on their angular separation, in a linear fashion. Such a measurement of the emission frequency as ϕ increases along the jet is clearly seen in the photometry of the jet in 3C 273 [14]. Furthermore, if the measurement is done at a single wavelength, intensity variation can be expected as the hotspot moves along the jet. In other words, measurements at higher wavelengths will find the peak intensities farther away from the core region, which is again consistent with observations.

F. Gamma Ray Bursts

The evolution of redshift of the thermal spectrum of a superluminal object also holds the explanation for gamma ray bursts (GRBs). γ ray bursts are short and intense flashes of γ rays in the sky, lasting from a few milliseconds to several minutes [15]. The short flashes (the prompt emissions) are followed by an after-glow of progressively softer energies. Thus, the initial γ rays are promptly replaced by X-rays, light and even radio frequency waves. This softening of the spectrum has been known for quite some time [16], and was first described using a hypernova (fireball) model. In this model, a relativistically expanding fireball produces the γ emission, and the spectrum softens as the fireball cools down [17]. The model calculates the energy released in the γ region as 10^{53} – 10^{54} ergs in a few seconds. This energy output is similar to about 1000 times the total energy released by the sun over its entire lifetime.

More recently, an inverse decay of the peak energy with varying time constant has been used to empirically fit the observed time evolution of the peak energy [18, 19] using a collapsar model. According to this model, GRBs are produced when the energy of highly relativistic flows in stellar collapses are dissipated, with the resulting radiation jets angled properly with respect to our line of sight. The collapsar model estimates a lower energy output, because the energy release is not isotropic, but concentrated along the jets. However, the rate of the collapsar events has to be corrected for the fraction of the solid angle within which the radiation jets can appear as GRBs. GRBs are observed roughly at the rate of once a day. Thus, the expected rate of the cataclysmic events powering the GRBs is of the order of 10^4 – 10^6 per day. Because of this inverse relationship between the rate and the estimated energy output, the total energy released per observed GRB remains the same.

Symmetric radio sources (galactic or extragalactic) and GRBs may appear to be completely distinct phenomena. However, their cores show a similar time evolution in the peak energy, but with very different time constants. Other similarities have begun to attract attention in the recent years [20]. Treating GRB as a manifestation of the light travel time results in a model that unifies these

two phenomena and makes detailed predictions of their kinematics.

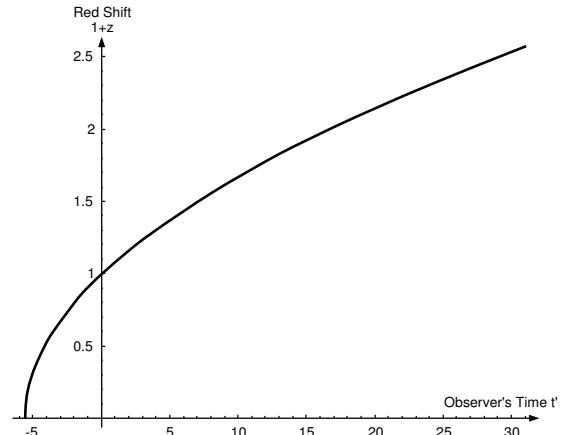


FIG. 5: Time evolution of the redshift from a superluminal object. It shows the redshifts expected from an object moving at $\beta = 300$ at a distance of ten million light years from us. The X axis is the observer's time in years. (Since the X axis scales with time, it is also the redshift from an object at 116 light days –ten million light seconds– with the X axis representing t_o in seconds.)

The spectra of GRBs rapidly evolve from γ region to an optical or even RF after-glow. This evolution is similar to the spectral evolution of the hotspots of a radio source as they move from the core to the lobes. The evolution of GRB can be made quantitative, because we know the dependence of the observer's time t_o and the redshift $1+z$ on the real time t (equations (3) and (5)). From these two, we can deduce the observed time evolution of the redshift (see Appendix A 6). We have plotted it parametrically in figure 5 that shows the variation of redshift as a function of the observer's time (t_o). The figure shows that the observed spectra of a superluminal object is expected to start at the observer's time $t_{o\min}$ with heavy (infinite) blue shift. The spectrum of the object rapidly softens and soon evolves to zero redshift and on to higher values. The rate of softening depending on its speed and distance from us. The speed and the distance are the only two parameters that are different between GRBs and symmetric radio sources in our model.

Note that the X axis in figure 5 scales with time. We have plotted an object with $\beta = 300$ and $y =$ ten million light years, with X axis is t_o in years. It is also the variation of $1+z$ for an object at $y =$ ten million light seconds (or 116 light days) with X axis in seconds. The former corresponds to symmetric jets and the latter to a GRB. Thus, for a GRB, the spectral evolution takes place at a much faster pace. Different combinations of β and y can be fitted to describe different GRB spectral evolutions.

To the observer, there is no object before $t_{o\min}$. In other words, there is a definite point in the observer's

time when the GRB is “born”, with no indication of its impending birth before that time. This birth does not correspond to any cataclysmic event (as would be required in the collapsar/hypernova or the “fireball” model) at the distant object. It is just an artifact of our perception.

In order to compare the time evolution of the GRB spectra to the ones reported in the literature, we need to get an analytical expression for the redshift (z) as a function of the observer’s time (t_o). This can be done by eliminating t from the equations for t_o and $1+z$ (equations (3) and (5)), with some algebraic manipulations as shown in Appendix A 6. The algebra can be made more manageable by defining $\tau = y/\beta$, a characteristic time scale for the GRB (or the radio source). This is the time the object would take to reach us, if it were coming directly toward us. We also define the age of the GRB (or radio source) as $t_{\text{age}} = t_o - t_{\text{omin}}$. This is just the observer’s time (t_o) shifted by the time at which the object first appears to him (t_{omin}). With these notations (and for small values t), it is possible to write the time dependence of z as:

$$1+z = \left| 1 + \frac{\beta^2 (-\tau \pm \sqrt{2\beta t_{\text{age}}})}{\beta t_{\text{age}} + \tau/2 \mp \sqrt{2\beta t_{\text{age}}} + \beta^2 \tau} \right| \quad (6)$$

for small values of $t \ll \tau$.

Since the peak energy of the spectrum is inversely proportional to the redshift, it can be written as:

$$E_{\text{pk}}(t_{\text{age}}) = \frac{E_{\text{pk}}(t_{\text{omin}})}{1 + C_1 \sqrt{\frac{t_{\text{age}}}{\tau}} + C_2 \frac{t_{\text{age}}}{\tau}} \quad (7)$$

where C_1 and C_2 are coefficients to be estimated by the Taylor series expansion of equation (6) or by fitting.

Ryde and Svensson [21] have studied the evolution of the peak energy ($E_{\text{pk}}(t)$), and modeled it empirically as:

$$E_{\text{pk}}(t) = \frac{E_{\text{pk},0}}{(1+t/\tau)^\delta} \quad (8)$$

where t is the time elapsed after the onset ($= t_{\text{age}}$ in our notation), τ is a time constant and δ is the hardness intensity correlation (HIC). Ryde and Svensson [21] reported seven fitted values of δ . We calculate their average as $\delta = 1.038 \pm 0.014$, with the individual values ranging from 0.4 to 1.1. Although it may not rule out or validate either model within the statistics, the δ reported may fit better to equation (7). Furthermore, it is not an easy fit, because there are too many unknowns. However, the similarity between the shapes of equations (7) and (8) is remarkable, and points to the agreement between our model and the existing data.

G. Expansion of the Universe

Our perception of superluminal motion also leads to the appearance of an expanding universe. The expansion

of the universe is inferred by the redshift measurements of recessional speeds. The apparent recessional speed is the longitudinal component of β_o is $\beta_{o\parallel} = \beta_o \cos \theta$. From equation (1), we can see that

$$\begin{aligned} \beta_{o\parallel} &= \beta_o \cos \theta = \frac{\beta \cos \theta}{1 - \beta \cos \theta} \\ \lim_{\beta \rightarrow \pm\infty} \beta_{o\parallel} &= -1 \end{aligned}$$

The apparent recessional speed tends to c (or, $\beta_{o\parallel} \rightarrow -1$), when the real speed is highly superluminal. This limiting value of $\beta_{o\parallel}$ is independent of the actual direction of motion of the object θ . Thus, whether a superluminal object is receding or approaching (or, in fact, moving in any other direction), its appearance from our perspective will be that of an object receding from us roughly at the speed of light.

The recessional speeds are measured using redshifts that, by equation (9), tend to large values as $\beta_{o\parallel} \rightarrow -1$.

$$\begin{aligned} 1+z &= \frac{1}{1 + \beta_o \cos \theta} \\ &= \frac{1}{1 + \beta_{o\parallel}} \end{aligned} \quad (9)$$

Thus, the appearance of all (possibly superluminal) objects receding from us at strictly subluminal speeds is an artifact of our perception, rather than the true nature of the universe.

H. Cosmic Microwave Background Radiation

The red shift of celestial objects $1+z$ also has an interesting limiting value at large angles, and for superluminal speeds.

$$\begin{aligned} 1+z &= |1 + \beta \sin \phi| \\ \lim_{\phi \rightarrow \pm\pi/2} 1+z &= |1 + \beta| \approx \beta \end{aligned}$$

Thus, if we picture our universe as a large number of superluminal or hyperluminal objects moving around in random directions, there will be a significant amount of low energy isotropic electromagnetic radiation. A low energy isotropic spectrum is remarkably similar to the cosmic microwave background radiation (CMBR). Thus, CMBR can be explained if we think of our visual reality as being limited by the light travel time effects. Note that it is not just our perception that gets fooled by the LTT effects, our measurement instruments also work at the speed of light and are subject to the same constraints.

V. CONCLUSIONS

In this article, we started with an insight from cognitive neuroscience about the nature of reality. Reality

is a convenient representation that our brain creates out of our sensory inputs. This representation, though convenient, is an incredibly distant experiential mapping of the actual physical causes that make up the inputs to our senses. Furthermore, limitations in the chain of sensing and perception map to measurable and predictable manifestations to the reality we perceive. One such fundamental constraint to our perceived reality is the speed of light, and the corresponding manifestations are generally termed the light travel time (LTT) effects. Because space and time are a part of a reality created out of light inputs to our eyes, some of their properties are manifestations of LTT effects, especially on our perception of motion. The absolute, physical reality generating the light inputs does not obey the properties we ascribe to our perceived space and time.

Noting that SR only considers frames of reference receding from each other, we showed that LTT effects are qualitatively identical. This similarity is not surprising because the coordinate transformation in SR is derived based partly on light travel time effects, and partly on the assumption that light travels at the same speed with respect to all inertial frames. In treating it as a manifestation of LTT, we did not address the primary motivation of SR, which is a covariant formulation of Maxwell's equations, as evidenced by the opening statements of Einstein's original paper [5]. It may be possible to disentangle the covariance of electrodynamics from the coordinate transformation, although it is not attempted in this article.

Unlike SR, LTT effects are asymmetric. This asymmetry provides a resolution to the twin paradox and an interpretation of the assumed causality violations associated with superluminality. Furthermore, the perception of superluminality is modulated by LTT effects, and explains γ ray bursts and symmetric jets. As we showed in the article, perception of superluminal motion also holds an explanation for cosmological phenomena like the expansion of the universe and cosmic microwave background radiation. The light travel time effects should be considered as a fundamental constraint in our perception, and consequently in physics, rather than as a convenient explanation for isolated phenomena.

Given that our perception is filtered through LTT effects, we have to deconvolute them from our perceived reality in order to understand the nature of the absolute, physical reality. This deconvolution, however, results in multiple solutions. Thus, the absolute, physical reality is beyond our grasp, and any *assumed* properties of the absolute reality can only be validated through how well the resultant *perceived* reality agrees with our observations. In this article, we assumed that the *absolute* reality obeys our intuitively obvious classical mechanics and asked the question how such a reality would be perceived when filtered through light travel time effects. We demonstrated that this particular treatment could explain certain astrophysical and cosmological phenomena that we observe.

The coordinate transformation in SR is a redefinition

of space and time (or, more generally, reality) in order to accommodate the distortions in our perception of motion due to light travel time effects. The absolute reality behind our perception is not subject to restrictions of SR. One may be tempted to argue that SR applies to the “real” space and time, not our perception. This line of argument begs the question, what is real? Reality is nothing but a cognitive model created in our brain starting from our sensory inputs, visual inputs being the most significant. Space itself is a part of this cognitive model. Perceptual constraints map directly to the nature of space as we perceive it. We have no access to a reality beyond our perception. The choice of accepting the perception of reality as a true image of reality and redefining space and time as described in special relativity indeed amounts to a philosophical choice. The alternative presented in the article is prompted by the view in modern neuroscience that reality is a cognitive model in the brain based on our sensory inputs. Adopting this alternative reduces us to guessing the nature of the absolute reality and comparing its predicted projection to our real perception. It may simplify and elucidate some theories in physics and explain some puzzling phenomena in our universe. However, this option is just another philosophical stance against the unknowable absolute reality.

APPENDIX A: MATHEMATICAL DETAILS

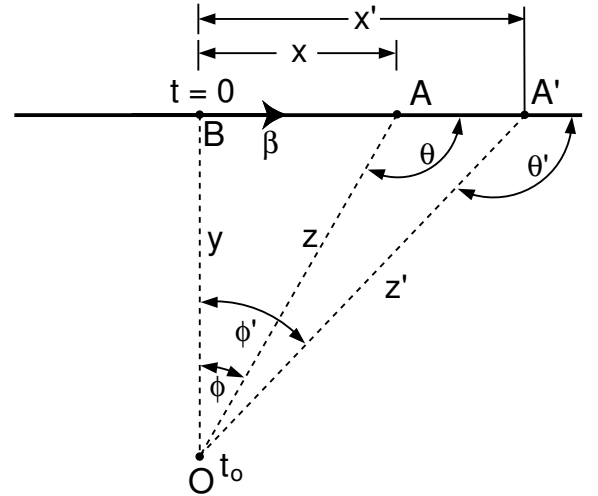


FIG. 6: The object is flying along BAA' , the observer is at O . The object crosses B (the point of closest approach) at time $t = 0$. It reaches A at time t . A photon emitted at A reaches O at time t_o , and a photon emitted at A' reaches O at time t_o' .

1. Perception of Speed

In this section, we derive how the perception of speed is distorted due to the light travel time (LTT) effects. We will show that the apparent speed is limited to the speed of light when the object is receding from us.

In figure 6, there is an observer at O . An object is flying by at a high speed $v = \beta c$ along the horizontal line BAA' . With no loss of generality, we can assume that $t = 0$ when the object is at B , the point of closest approach. It passes A at time t . The photon emitted at time $t = 0$ reaches the observer at time $t = t_o$, and the photon emitted at A' (at time $t = t'$) reaches him at time $t = t_o'$. The angle between the object's velocity at A and the observer's line of sight is θ . We have the Pythagoras equations:

$$\begin{aligned} z^2 &= x^2 + y^2 \\ z'^2 &= x'^2 + y^2 \\ \Rightarrow \frac{x + x'}{z + z'} &= \frac{z - z'}{x - x'} \end{aligned} \quad (A1)$$

If we assume that x and z (distances at time t_0) are not very different from x' and z' respectively (distances at time t_o), we can write,

$$-\cos \theta = \sin \phi = \frac{x}{z} \approx \frac{x' + x}{z' + z} = \frac{z' - z}{x' - x} \quad (A2)$$

We define the real speed of the object as:

$$v = \beta c = \frac{x' - x}{t' - t} \quad (A3)$$

But the speed it *appears* to have will depend on when the observer senses the object at A and A' . The apparent speed of the object is:

$$v' = \beta_o c = \frac{x' - x}{t_o' - t_o} \quad (A4)$$

We also have

$$\begin{aligned} t_o &= t + \frac{z}{c} \\ t_o' &= t' + \frac{z'}{c} \\ \Rightarrow t_o' - t_o &= t' - t + \frac{z' - z}{c} \end{aligned} \quad (A5)$$

Thus,

$$\begin{aligned} \frac{\beta}{\beta_o} &= \frac{t_o' - t_o}{t' - t} \\ &= 1 + \frac{z' - z}{c(t' - t)} \\ &= 1 - \frac{x - x'}{c(t' - t)} \cos \theta \\ &= 1 - \beta \cos \theta \end{aligned} \quad (A6)$$

which gives,

$$\begin{aligned} \beta_o &= \frac{\beta}{1 - \beta \cos \theta} \\ \beta &= \frac{\beta_o}{1 + \beta_o \cos \theta} \end{aligned} \quad (A7)$$

and,

$$\begin{aligned} \frac{\beta_o}{\beta} &= \frac{1}{1 - \beta \cos \theta} \\ &= 1 + \beta_o \cos \theta \\ &= \sqrt{\frac{1 + \beta_o \cos \theta}{1 - \beta \cos \theta}} \end{aligned} \quad (A8)$$

LTT effects modulate the way we perceive time at objects in motion. Here we show that a receding object appears to have a dilated time flow. From figure 6, we can see that $\theta = \pi$ for an object receding from the observer. Thus, the apparent speed of a receding object is:

$$\begin{aligned} \beta_o &= \frac{\beta}{1 + \beta} \\ \lim_{\beta \rightarrow \pm\infty} \beta_o &= 1 \end{aligned} \quad (A9)$$

Thus, an object can never appear to be receding faster than the speed of light.

2. Time Dilation

Referring to figure 6, we can see that the real time elapsed as the object moves from A to A' is:

$$\Delta t = t' - t \quad (A10)$$

This time period appears to the observer as:

$$\Delta t_o = t_o' - t_o \quad (A11)$$

Using the definitions of the real and apparent speeds as in equations (A3) and (A4), we can write:

$$\begin{aligned} \frac{\Delta t_o}{\Delta t} &= \frac{\beta}{\beta_o} \\ &= 1 - \beta \cos \theta \\ &= \frac{1}{1 + \beta_o \cos \theta} \end{aligned} \quad (A12)$$

where we used the known relationship between β and β_o from equation (A8).

For an object receding from the observer, $\theta = \pi$ and the equation becomes:

$$\frac{\Delta t_o}{\Delta t} = \frac{1}{1 - \beta_o} \quad (A13)$$

For an object approaching the observer, $\theta = 0$ and the equation becomes:

$$\frac{\Delta t_o}{\Delta t} = \frac{1}{1 + \beta_o} \quad (A14)$$

This shows a time contraction, instead of a time dilation.

3. Length Contraction

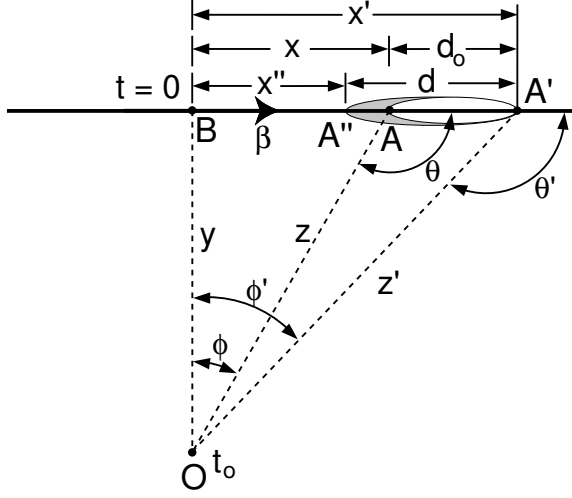


FIG. 7: The object has a real length of d , and is shown as the shaded ellipse. To the observer at O , it appears to have a length of d_o due to LTT effects.

The perceived length of an object in motion is affected due to LTT effects. In particular, a receding object appears shorter. In figure 7, we have the object of real length d . The perceived length of the object is the distance between the leading edge and the trailing edge from which the photons reach the observer at the same instant. In figure 7, it is denoted by d_o . The photon emitted from the trailing edge of the object when it is at x reaches the observer at O at time t_o . At the same time, a photon from the leading edge at x' reaches O . But, when the leading edge is at x' , the trailing edge is only at $x'' = x' - d$, due to the motion.

Since the object's speed is v and the time starts when the object passes B , we can write:

$$\begin{aligned} t_o &= \frac{x}{v} + \frac{z}{c} \\ &= \frac{x''}{v} + \frac{z'}{c} \\ &= \frac{x' - d}{v} + \frac{z'}{c} \end{aligned} \quad (\text{A15})$$

Using the equation for the apparent length of the object $d_o = x' - x$, we can rewrite this as:

$$\begin{aligned} \frac{z' - z}{c} &= \frac{x - x' + d}{v} \\ &= \frac{d - d_o}{v} \end{aligned} \quad (\text{A16})$$

The approximation for $\cos \theta$ in equation (A2) is still valid, with the additional information that the apparent length

of the object $d_o = x' - x$.

$$-\cos \theta = \frac{z' - z}{d_o} \quad (\text{A17})$$

Thus, equation (A16) becomes:

$$-d_o \cos \theta = \frac{d - d_o}{\beta} \quad (\text{A18})$$

Or,

$$\begin{aligned} \frac{d_o}{d} &= \frac{1}{1 - \beta \cos \theta} \\ &= 1 + \beta_o \cos \theta \\ &= \frac{\beta_o}{\beta} \end{aligned} \quad (\text{A19})$$

For an object receding from the observer, $\theta = \pi$ and the equation becomes:

$$\frac{d_o}{d} = 1 - \beta_o \quad (\text{A20})$$

For an object approaching the observer, $\theta = 0$ and the equation becomes:

$$\frac{d_o}{d} = 1 + \beta_o \quad (\text{A21})$$

which shows that the apparent length of the object is greater than its real length.

4. Doppler Shift

Redshift (z) defined as:

$$1 + z = \frac{\lambda_o}{\lambda} \quad (\text{A22})$$

where λ_o is the measured wavelength and λ is the known wavelength. In figure 6, the number of wave cycles created in time $t' - t$ between A and A' is the same as the number of wave cycles sensed at O between t_o' and t_o . Substituting the values, we get:

$$\frac{(t' - t)c}{\lambda} = \frac{(t_o' - t_o)c}{\lambda_o} \quad (\text{A23})$$

Using the definitions of the real and apparent speeds from equations (A3) and (A4), it is easy to get:

$$\frac{\lambda_o}{\lambda} = \frac{\beta}{\beta_o} \quad (\text{A24})$$

Using the relationship between the real speed β and the apparent speed β_o from equation (A8), we get:

$$\begin{aligned} 1 + z &= \frac{1}{1 + \beta_o \cos \theta} \\ &= 1 - \beta \cos \theta \end{aligned} \quad (\text{A25})$$

As expected, z depends on the longitudinal component of the velocity of the object. Since we allow superluminal speeds in this calculation, we need to generalize this equation for z noting that the ratio of wavelengths is positive. Taking this into account, we get:

$$1 + z = \left| \frac{1}{1 + \beta_o \cos \theta} \right| = |1 - \beta \cos \theta| \quad (\text{A26})$$

For a receding object $\theta = \pi$. If we consider only subluminal speeds, we can rewrite this as:

$$1 + z = \sqrt{\frac{1 + \beta}{1 - \beta}} \quad (\text{A27})$$

If we were to mistakenly assume that the speed we observe is the real speed, then this becomes the relativistic Doppler formula:

$$1 + z = \sqrt{\frac{1 + \beta}{1 - \beta}} \quad (\text{A28})$$

5. Kinematics of Superluminal Objects

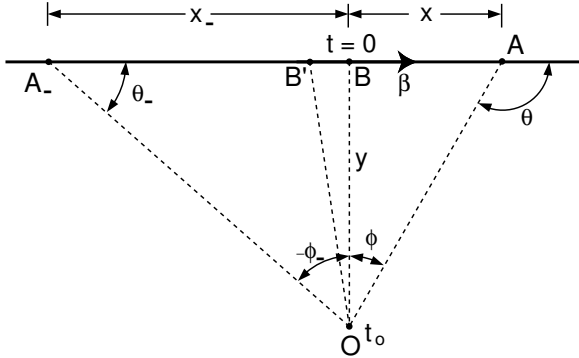


FIG. 8: An object flying along A_-BA at a constant superluminal speed. The observer is at O . The object crosses B (the point of closest approach to O) at time $t = 0$.

The derivation of the kinematics is based on figure 8. Here, an object is moving at a superluminal speed along A_-BA . At the point of closest approach, B , the object is a distance of y from the observer at O . Since the speed is superluminal, the light emitted by the object at some point B' (before the point of closest approach B) reaches the observer *before* the light emitted at A_- . This gives an illusion of the object moving in the direction from B' to A_- , while in reality it is moving from A_- to B' .

ϕ is the observed angle with respect to the point of closest approach B . ϕ is defined as $\theta - \pi/2$ where θ is the angle between the object's velocity and the observer's

line of sight. ϕ is negative for negative time t . We choose units such that $c = 1$, in order to make algebra simpler. t_o denotes the observer's time. Note that, by definition, the origin in the observer's time, t_o is set to the instant when the object appears at B .

The real position of the object at any time t is:

$$x = y \tan \phi = \beta t \quad (\text{A29})$$

Or,

$$t = \frac{y \tan \phi}{\beta} \quad (\text{A30})$$

A photon emitted by the object at A (at time t) will reach O after traversing the hypotenuse. A photon emitted at B will reach the observer at $t = y$, since we have chosen $c = 1$. If we define the observer's time t_o such that the time of arrival is $t = t_o + y$, then we have:

$$t_o = t + \frac{y}{\cos \phi} - y \quad (\text{A31})$$

which gives the relation between t_o and ϕ .

$$t_o = y \left(\frac{\tan \phi}{\beta} + \frac{1}{\cos \phi} - 1 \right) \quad (\text{A32})$$

Expanding the equation for t_o to second order, we get:

$$t_o = y \left(\frac{\phi}{\beta} + \frac{\phi^2}{2} \right) \quad (\text{A33})$$

The minimum value of t_o occurs at $\phi_0 = -1/\beta$ and it is $t_{o\min} = -y/2\beta^2$. To the observer, the object first appears at the position $\phi = -1/\beta$. Then it appears to stretch and split, rapidly at first, and slowing down later.

The quadratic equation (A33) can be recast as:

$$1 + \frac{2\beta^2}{y} t_o = (1 + \beta\phi)^2 \quad (\text{A34})$$

which will be more useful later in the derivation.

The angular separation between the objects flying away from each other is the difference between the roots of the quadratic equation (A33):

$$\begin{aligned} \Phi &= \phi_1 - \phi_2 \\ &= \frac{2}{\beta} \sqrt{1 + \frac{2\beta^2}{y} t_o} \\ &= \frac{2}{\beta} (1 + \beta\phi) \end{aligned} \quad (\text{A35})$$

making use of equation (A34). Thus, we have the angular separation either in terms of the observer's time ($\Phi(t_o)$) or the angular position of the object ($\Phi(\phi)$) as illustrated in Figure 9.

The rate at which the angular separation occurs is:

$$\begin{aligned} \frac{d\Phi}{dt_o} &= \frac{2\beta}{y \sqrt{1 + \frac{2\beta^2}{y} t_o}} \\ &= \frac{2\beta}{y (1 + \beta\phi)} \end{aligned} \quad (\text{A36})$$

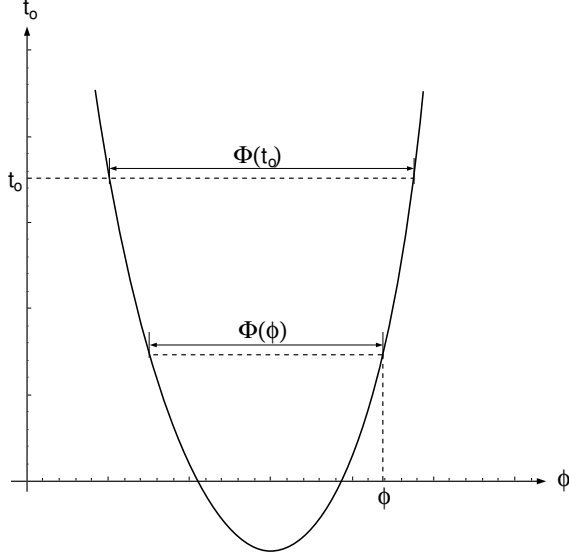


FIG. 9: Illustration of how the angular separation is expressed either in terms of the observer's time ($\Phi(t_o)$) or the angular position of the object ($\Phi(\phi)$)

Again, making use of equation (A34). Defining the apparent age of the radio source $t_{\text{age}} = t_o - t_{\text{omin}}$ and knowing $t_{\text{omin}} = -y/2\beta^2$, we can write:

$$\begin{aligned}
 \frac{d\Phi}{dt_o} &= \frac{2\beta}{y\sqrt{1 + \frac{2\beta^2}{y}t_o}} \\
 &= \frac{2\beta}{y\sqrt{1 - \frac{t_o}{t_{\text{omin}}}}} \\
 &= \sqrt{\frac{4\beta^2}{y^2}} \times \frac{-t_{\text{omin}}}{t_o - t_{\text{omin}}} \\
 &= \sqrt{\frac{2}{y t_{\text{age}}}} \quad (\text{A37})
 \end{aligned}$$

6. Time Evolution of the Redshift

As shown before in equation (A26), the redshift z depends on the real speed β as:

$$1 + z = |1 - \beta \cos \theta| = |1 + \beta \sin \phi| \quad (\text{A38})$$

For any given time (t_o) for the observer, there are two solutions for ϕ and z . ϕ_1 and ϕ_2 lie on either side of $\phi_0 = 1/\beta$. For $\sin \phi > -1/\beta$, we get

$$1 + z_2 = 1 + \beta \sin \phi_1 \quad (\text{A39})$$

and for $\sin \phi < -1/\beta$,

$$1 + z_1 = -1 - \beta \sin \phi_2 \quad (\text{A40})$$

Thus, we get the difference in the redshift between the two hotspots at ϕ_1 and ϕ_2 as:

$$\Delta z \approx 2 + \beta(\phi_1 + \phi_2) \quad (\text{A41})$$

We also have the mean of the solutions of the quadratic (ϕ_1 and ϕ_2) equal to the position of the minimum (ϕ_0):

$$\frac{\phi_1 + \phi_2}{2} = -\frac{1}{\beta} \quad (\text{A42})$$

Thus $\phi_1 + \phi_2 = -2/\beta$ and hence $\Delta z = 0$. The two hotspots will have identical redshifts, if terms of ϕ^3 and above are ignored.

As shown before (see equation (A38)), the redshift z depends on the real speed β as:

$$1 + z = |1 + \beta \sin \phi| = \left| 1 + \frac{\beta^2 t}{\sqrt{\beta^2 t^2 + y^2}} \right| \quad (\text{A43})$$

Since we know z and t_o functions of t , we can plot their inter-dependence parametrically. This is shown in figure 5 of the article.

It is also possible to eliminate t and derive the dependence of $1 + z$ on the apparent age of the object under consideration, $t_{\text{age}} = t_o - t_{\text{min}}$. In order to do this, we first define a time constant $\tau = y/\beta$. This is the time the object would take to reach us, if it were flying directly toward us. First, let's get an expression for t/τ :

$$\begin{aligned}
 t_o &= t + \sqrt{\beta^2 t^2 + y^2} - y \\
 &= t + \beta\tau \sqrt{1 + \frac{t^2}{\tau^2}} - \beta\tau \\
 &\approx t + \frac{\beta t^2}{2\tau} \\
 \Rightarrow \frac{t}{\tau} &= \frac{-1 \pm \sqrt{1 + \frac{2\beta t_{\text{age}}}{\tau}}}{\beta} \quad (\text{A44})
 \end{aligned}$$

Note that this is valid only for $t \ll \tau$. Now we collect the terms in t/τ in the equation for $1 + z$:

$$\begin{aligned}
 t_o &= t + \sqrt{\beta^2 t^2 + y^2} - y \\
 \Rightarrow \sqrt{\beta^2 t^2 + y^2} &= t_o - t + y \\
 1 + z &= \left| 1 + \frac{\beta^2 t}{\sqrt{\beta^2 t^2 + y^2}} \right| \\
 &= \left| 1 + \frac{\beta^2 t}{t_o - t + y} \right| \\
 &= \left| 1 + \frac{\beta^2 \frac{t}{\tau}}{\frac{t_{\text{age}}}{\tau} - \frac{1}{2\beta} - \frac{t}{\tau} + \beta} \right| \quad (\text{A45})
 \end{aligned}$$

As expected, the time variables always appear as ratios like t/τ , giving confidence that our choice of the characteristic time scale is probably right. Finally, we can substitute t/τ from equation (A44) in equation (A45) to obtain:

$$1 + z = \left| 1 + \frac{\beta^2 (-\tau \pm \sqrt{2\beta t_{\text{age}}})}{\beta t_{\text{age}} + \tau/2 \mp \sqrt{2\beta t_{\text{age}}} + \beta^2 \tau} \right| \quad (\text{A46})$$

7. Estimating Real Speed from Apparent Speed

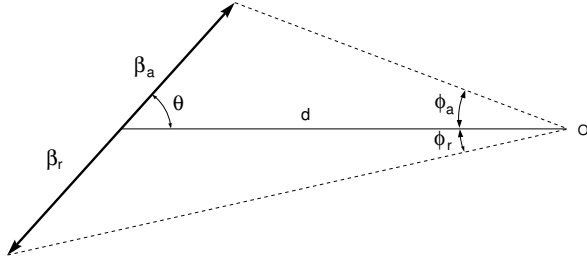


FIG. 10: Illustration of the real jet speeds (β_a and β_r), core distance (d) and the angles.

In the traditional explanation of superluminality, superluminal objects such as GRS 1915+105 are assumed to be two jets emanating from a core. The axis of the jets makes an angle θ with respect to our line of sight. The only direct kinematic measurements we have are the angular velocities of features (or knots) in the jets. We have two angular rates, μ_a and μ_r , for the approaching and receding jets. The distance of the core from us (d) is not known. Also unknown are the real speeds of the jets β_a and β_r , which are usually assumed to be the same (β). The apparent transverse speeds ($\beta_{o\perp}^a$ and $\beta_{o\perp}^r$) are different for the two jets. Thus, we have the following definitions:

$$\mu_a = \frac{d\phi_a}{dt_o} \quad (\text{A47})$$

$$\mu_r = \frac{d\phi_r}{dt_o} \quad (\text{A48})$$

$$\beta_{o\perp}^a = \mu_a d \quad (\text{A49})$$

$$\beta_{o\perp}^r = \mu_r d \quad (\text{A50})$$

where t_o is our time. Assuming the real jet speeds are the same ($\beta_a = \beta_r = \beta$) and using the relationship between β and β_o from equation (A8), we have the following equations:

$$\mu_a d = \frac{\beta \sin \theta}{1 - \beta \cos \theta} \quad (\text{A51})$$

$$\mu_r d = \frac{\beta \sin \theta}{1 + \beta \cos \theta} \quad (\text{A52})$$

There are three unknowns (β , θ and d) and only two equations. Thus, it is always possible to impose the relativistic condition ($\beta < 1$) and compute corresponding limits on θ and d . The only way to estimate the real speed or the angle is to have an independent (and, hopefully, model-independent) measurement of d .

In order to find the limiting values of $\beta_{o\perp}^a$ and $\beta_{o\perp}^r$, we set $\beta \rightarrow 1$ in equations (A51) and (A52).

$$\beta_{o\perp}^a = \frac{\sin \theta}{1 - \cos \theta} \quad (\text{A53})$$

$$\beta_{o\perp}^r = \frac{\sin \theta}{1 + \cos \theta} \quad (\text{A54})$$

Or,

$$\beta_{o\perp}^a = \frac{\sin \theta}{1 - \cos \theta} \quad (\text{A55})$$

$$= \frac{\sqrt{1 - \cos^2 \theta}}{1 - \cos \theta} \quad (\text{A56})$$

$$= \frac{\sqrt{(1 - \cos \theta)(1 + \cos \theta)}}{1 - \cos \theta} \quad (\text{A57})$$

$$= \sqrt{\frac{1 + \cos \theta}{1 - \cos \theta}} \quad (\text{A58})$$

$$= \sqrt{\frac{(1 + \cos \theta)(1 + \cos \theta)}{(1 - \cos \theta)(1 + \cos \theta)}} \quad (\text{A59})$$

$$= \frac{1 + \cos \theta}{\sqrt{1 - \cos^2 \theta}} \quad (\text{A60})$$

$$= \frac{1 + \cos \theta}{\sin \theta} \quad (\text{A61})$$

$$= \frac{1}{\beta_{o\perp}^r} \quad (\text{A62})$$

Thus, if we assume that the real speeds are limited to $\beta < 1$, the apparent transverse speed of the receding jet ($\beta_{o\perp}^r$) is limited to the reciprocal of the apparent transverse speed of the approaching jet ($\beta_{o\perp}^a$). As long as the measured angular speeds of the two jets are different, one can always find an estimated distance such that the reciprocal inequality holds, because the system of equations is under-constrained.

-
- [1] V. S. Ramachandran, *The Emerging Mind: Reith Lectures on Neuroscience* (BBC, 2003).
 - [2] L. M. Chen, R. M. Friedman, and A. W. Roe1, *Science* **302**, 881 (2003).
 - [3] J. A. Biretta, W. B. Sparks, and F. Macchetto, *ApJ* **520**, 621 (1999).
 - [4] A. J. Zensus, *ARA&A* **35**, 607 (1997).
 - [5] A. Einstein, *Annalen der Physik* **17**, 891 (1905).
 - [6] I. F. Mirabel and L. F. Rodríguez, *Nature* **371**, 46 (1994).

- [7] I. F. Mirabel and L. F. Rodríguez, *ARA&A* **37**, 409 (1999).
- [8] G. Gisler, *Nature* **371**, 18 (1994).
- [9] R. P. Fender, S. T. Garrington, D. J. McKay, T. W. B. Muxlow, G. G. Pooley, R. E. Spencer, A. M. Stirling, and E. B. Waltman, *MNRAS* **304**, 865 (1999).
- [10] M. Rees, *Nature* **211**, 468 (1966).
- [11] R. A. Perley, J. W. Dreher, and J. J. Cowan, *ApJ* **285**, L35 (1984).

- [12] I. Owsianik and J. E. Conway, *A&A* **337**, 69 (1998).
- [13] A. G. Polatidis, J. E. Conway, and I. Owsianik, in *Proceedings of the 6th European VLBI Network Symposium*, edited by Ros, Porcas, Lobanov, Zensus (2002).
- [14] S. Jester, H. J. Roeser, K. Meisenheimer, and R. Perley, *A&A* **431**, 477 (2005), astro-ph/0410520.
- [15] T. Piran, *International Journal of Modern Physics A* **17**, 2727 (2002).
- [16] E. P. Mazets, S. V. Golenetskii, V. N. Ilyinskii, Y. A. Guryan, and R. L. Aptekar, *Ap&SS* **82**, 261 (1982).
- [17] T. Piran, *Phys.Rept.* **314**, 575 (1999).
- [18] F. Ryde, *ApJ* **614**, 827 (2005).
- [19] F. Ryde, , and R. Svensson, *ApJ* **566**, 210 (2003).
- [20] G. Ghisellini, *J.Mod.Phys.A* (Proceedings of 19th European Cosmic Ray Symposium - ECRS 2004) (2004), astro-ph/0411106.
- [21] F. Ryde and R. Svensson, *ApJ* **529**, L13 (2000).